

PREDICTING ENERGY LOSSES CAUSED BY POWER LINE-VEGETATION CONFLICT

N. Bahador¹ A.E. Ashrafi² A.H. Lotfi² S. Chatrazar²

1: Lorestan University

2: Electricity Distribution Company of Hamedan

Abstract: Most of overhead distribution networks in urban and rural areas of world are in interfering with trees which lead to power losses. This paper studies the effective factors in power losses caused by vegetation and proposes a new model for power loss based on finite element method so that wholly reflects the impacts of environmental conditions and biological classification. In suggested algorithm, the effects of species, temperature, humidity and seasonal variations on the power loss estimation are fully considered. Experimental investigations on a low voltage distribution network verify the proposed method's operation.

Key words: Energy Losses Prediction, Numerical Modeling, 2D Finite element method, LV Distribution Systems.

1. Introduction

Performance evaluation of power systems is of interest to all power engineers. Power losses estimation is essential part of this evaluation. Part of these losses are related to the growth of trees beside power lines (Figure 1). Despite the fact that the first need for the reduction of tree losses is an accurate evaluation, a detailed study has not been done in this field thus far.



Fig. 1. Constant contact of Plane tree with low voltage network, Hamedan/Iran.

The accurate and low time-consuming estimation of the power losses in distribution networks is extremely important for achieving systems with higher efficiency and reliability [1-3].

The tree overgrowth near power lines leads to leaking electrical current. Despite the low value of this leakage, placing trees continuously next to energized conductors, results in significant annual losses which have not been taken under consideration.

Despite the importance of this issue, no accurate method for estimation of these losses has been presented thus far in which all the effects of species, temperature, humidity and seasonal variations on the power loss were fully considered.

Previous researches in the field of trees-power line conflicts have not considered power loss and just focused on detection and location of it as high impedance fault on medium voltage systems [4-7]. As shown in table 1, the results of two different researches in HIF current measurement are also incompatible with each other. This shows that tree-related power loss is a variable parameter which depends on different factors. Therefore, due to importance of power losses issue in distribution networks, using the results of precise measurement and accurate estimation of losses considering all effective factors can provide solutions for future decisions.

Table 1. Current drawn by pine tree in contact with 20 kv conductor [8, 9]

20 kV power line	
100 mA	0.9 – 2.2 mA

Based on measurements taken on the trees touching LV power lines [8], the internal structure of trees and consequently the amount of leakage current passes through them changes in short-term environmental conditions (temperature and humidity) and long-term environmental conditions (seasonal variation in tree physiology). Furthermore, the effect of moisture content variations on electrical resistance is not the same for all species [8]. Considering the factors mentioned above, this research presents a finite element-based algorithm for vegetation-related power loss estimation.

2. The experimental tests on low voltage network

A series of experiments were carried out in different seasons (spring, summer and autumn) to verify hypothesis of losses impressionability from the seasonal variations in in physiology. The experiments were conducted on-site on live trees grown next to the 380 volt distribution network in Hamendan, Iran. The tested species included Pine, Ash, Plane and Acacia. Figure 2 shows the tested ash tree. Testing Procedure was as follow: Short piece of cooper conductor had touched the power line and providing connection to tree (Figure 1). As minimum leakage current was in the 100 nanometer regime, to accurately measure the total leakage flowing to the intended connection, a micrometer measurement device with accuracy of 0.1 μ A (Model VC97) had been placed in series with conductor. The variations of leakage current value were studied in different weather and seasonal conditions and summarized in figure 3.



Fig. 2. Limb's direct connection to S-phase of 380 volt network (Ash tree)

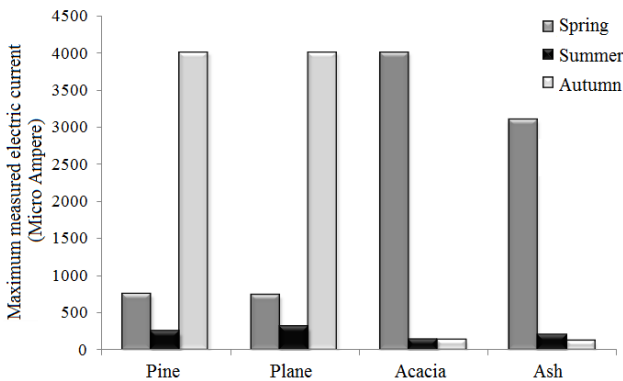


Fig. 3. Maximum value of measured leakage current in tested trees over seasons

Broad-leaf trees in terms of vessels are divided into

three classes, semi-ring porous species, diffuse porous species and ring porous species. The wood of ring porous species are divided into two categories, spring wood (early wood) with wider vascular channel and thinner vascular wall which formed during spring season, and autumn wood (or late wood) with narrow vascular channel and thicker vascular wall which formed during autumn season. So ring porous trees do not have the same vascular sections during spring and autumn. While there is no significant difference between vascular sections in diffuse porous trees during spring and autumn. Among tested trees, Plane places in diffuse porous group and that is why its vascular sections in spring, summer and autumn are same. So maximum transferred water in its vessels is same in all seasons. According to this point and with regard to this fact that autumn is the most humid season in Hamadan, it can be concluded that the maximum and minimum leakage current of Plane is occurred in autumn and summer respectively. Unlike the Plane, the transferred water in vessels of Ash and Acacia which placed in ring porous species and consequently their leakage current are maximum and minimum in spring and autumn respectively. In conifers such as Pine, there is no considerable difference between tracheids of spring wood and autumn wood [8]. So, changes in maximum leakage current follow the same pattern of Plane. Test results in figures confirm the above assumptions.

3. Impressibility of tree moisture content from environment

Placing a tree in an environment, results in moisture exchange between air and tree. Tree moisture content is a function of temperature and humidity and calculated using the following formula [11].

$$MC = \frac{1800}{W} \left[\frac{kh}{1 - kh} + \frac{k_1 kh + 2k_1 k_2 k^2 h^2}{1 + k_1 kh + k_1 k_2 k^2 h^2} \right] \quad (1)$$

Where

MC = moisture content (%)

h = relative humidity (%/100)

For the temperature in degrees Celsius (T_c), Values of W, k, k_1 and k_2 in equation (1) are also obtained using the following relations.

$$\begin{aligned} W &= 349 + 1.29T_c + 0.0135T_c^2 \\ k &= 0.805 + 0.000736T_c - 0.00000273T_c^2 \\ k_1 &= 6.27 - 0.00938T_c - 0.000303T_c^2 \\ k_2 &= 1.91 + 0.0407T_c - 0.000293T_c^2 \end{aligned} \quad (2)$$

4. Relation between electrical resistance and moisture content

The electrical resistance of trees is affected by several factors, including tree species, temperature and humidity of environment [8]. Therefore, each species has its own electrical characteristics. Figure 4 shows electrical resistance-moisture content characteristics of the sample trees, including pine, spruce, beech, birch, larch and oak.

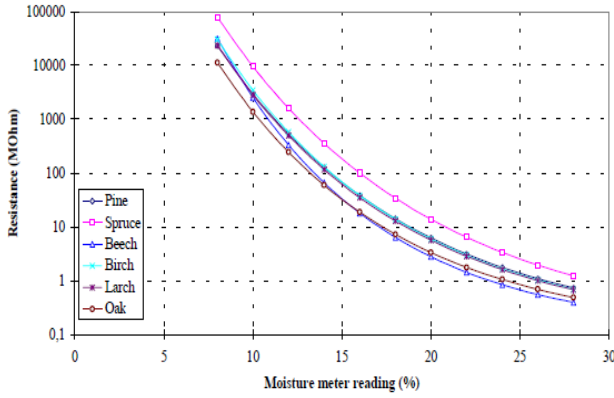


Fig. 4. Electrical resistance-moisture content characteristics of some tree species [10]

Table 2. Regression coefficients (Samuelsson model) [11]

Species	N° samples	Parallel to the grain (Rp)		R ²
		a	b	
Beech	36	-0.046722 ± 0.000579	1.12606 ± 0.008708	0.994
<i>Fagus sylvatica</i>				
European white oak	36	-0.046368 ± 0.000597	1.07042 ± 0.007946	0.994
<i>Quercus robur</i>				
American red oak	36	-0.045562 ± 0.000508	1.11785 ± 0.006794	0.995
<i>Quercus rubra</i>				
American white oak	36	-0.0514145 ± 0.000899	1.16365 ± 0.011588	0.989
<i>Quercus alba</i>				
American ash	36	-0.051567 ± 0.000621	1.13545 ± 0.009242	0.995
<i>Fraxinus sp.</i>				
American chestnut	36	-0.0393465 ± 0.000775	1.0294 ± 0.011427	0.987
<i>Castanea dentata</i>				
Iroko/African teak	36	-0.07511565 ± 0.001854	1.33626 ± 0.022151	0.979
<i>Chlorophora excelsa</i>				
American cherry	27	-0.0467145 ± 0.001164	1.13123 ± 0.013117	0.983
<i>Prunus serotina</i>				
Limba/White afara	35	-0.0480084 ± 0.000790	1.10629 ± 0.011088	0.991
<i>Terminalia superba</i>				
Samba/Obeche	19	-0.0539734 ± 0.000976	1.16087 ± 0.012704	0.994
<i>Triplochiton scleroxylon</i>				

Logarithmic model used in this paper, is Samuelson model proposed in 1990 that shows the relation between electrical resistance (in mega ohms) with moisture content (in percentage terms) with the following equation.

$$\text{Log} [\text{Log}(R) + 1] = a.h + b \quad (3)$$

Where R is the electrical resistance of tree in terms of mega-ohms, a and b are coefficients of the model.

Equation (3) has been proved to be in conformity with experimental data and extensively used in studies of other researchers. Furthermore, the values of coefficients a and b are precisely obtained for different species in numerous studies. For instance, the values of these coefficients for some trees are listed in Table 2.

5. Estimation of the leakage current in various tree species

To consider long-term environmental conditions in calculations, the tomography imagery of each season will be used. Using tomography imagery, the initial resistivity of tree in each season is obtained. This resistance is assigned to a specific environmental condition by which the initial moisture content of tree (MC₀) is achieved. So for each season, there will be an initial resistivity at initial moisture content.

According to Eq 3, the electrical resistance can be calculated based on corresponding moisture content.

$$R = 10^{(10^{a \cdot MC + b} - 1)} \quad (4)$$

Values of coefficients of relation 4 are selected according to studied species. According to constant dimensions of tree and based on Eq 4, tree resistivity is proportional to tree electrical resistance.

$$\rho \propto R \propto 10^{(10^{a \cdot MC + b} - 1)} \quad (5)$$

Regarding Eq 5 and initial resistivity derived from tomography images (ρ_1) and according to moisture content of tree, resistivity value corresponding to specified environmental conditions is estimated using the following equation. This obtained resistivity is applied to finite element analysis as input data and the power loss of tree is calculated (Figure 5).

$$\rho_2 = \rho_1 \left[\frac{10^{(10^a \cdot MC_2 + b - 1)}}{10^{(10^a \cdot MC_1 + b - 1)}} \right] \quad (6)$$

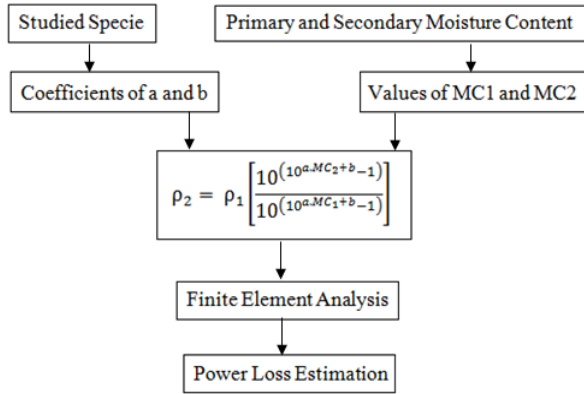


Fig. 5. Flowchart of power losses estimation process

6. Power Loss estimation of tree contact with low voltage network

Since tree contacting with network has a three-dimensional structure, taking into account the third dimension in modeling leads to more accurate solutions. But due to large dimensions and heterogeneous structure (small diameter of tree trunk cross-section compared to its height), there is limitation to create fine meshes for the purpose of accurate calculations. Two dimensional simulation will also provide quicker results. That's why this section studies the contact of ash tree with low voltage network through two-dimensional analysis.

For modeling, the distribution of electrical resistivity along cross-section of ash tree is first extracted based on tomography image. In tomography image (figure 6), the blue points which represent the trunk rot are not considered in the simulation.

To employ the variation of electrical resistivity along tree cross-section, the trunk is divided into 14 sections and each section is assigned one specific resistivity. Figure 7 shows the electrical resistivity profile over different parts of the trunk. It should be noted that these electrical resistivity values are related to moisture content of 1.9 percent in the spring season. To apply the finite element method to model, the resistivity values should be converted into values in given

conditions according to the proposed algorithm.

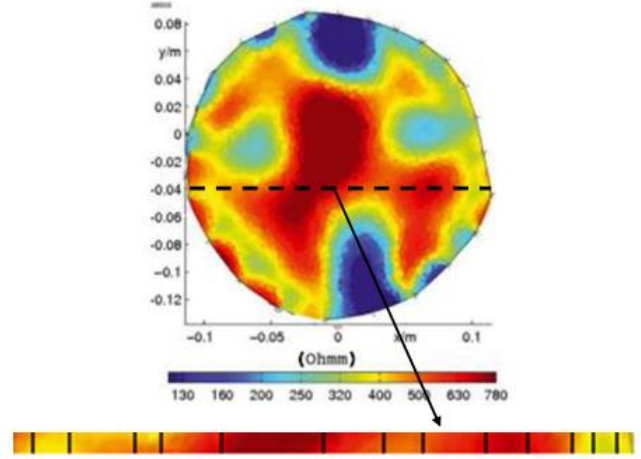


Fig. 6. Dividing ash cross-sections into 14 separate sections

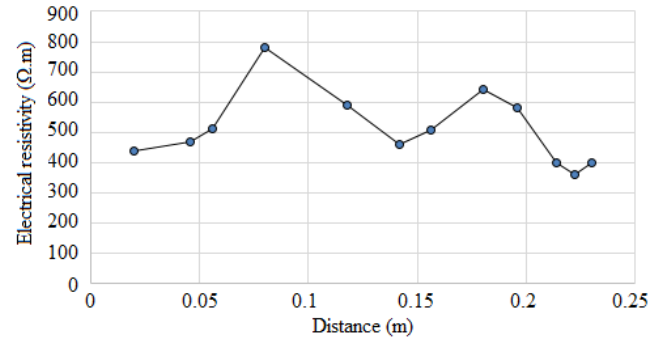


Fig. 7. Electrical resistivity profile along ash cross-section at the moisture content of 9.1 %

Figure 8 shows two-dimensional meshed model of tree contact with power line. To increase the accuracy of calculations, very fine meshes are considered. Figure 9 is a zoom of meshed sections of trunk with different resistivity.

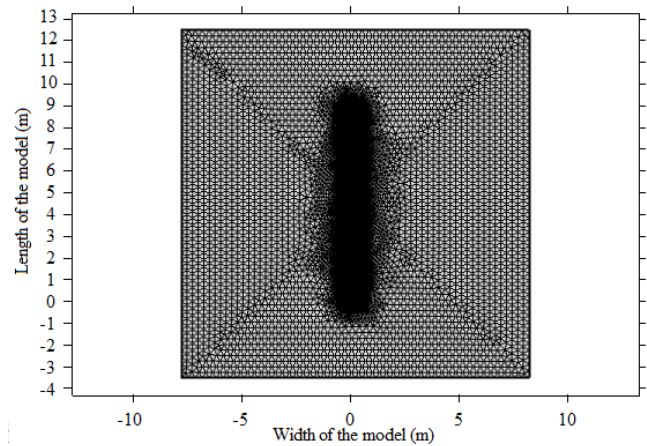


Fig. 8. Two-dimensional meshed model of tree-power line contact

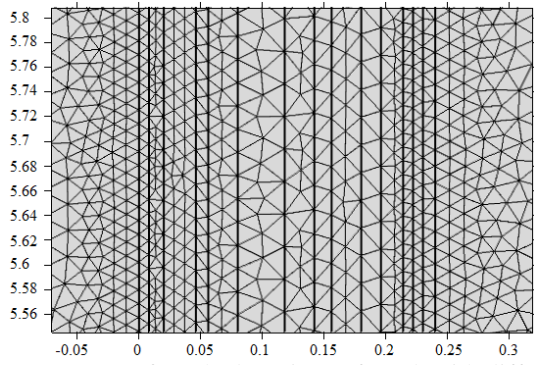


Fig. 9. A zoom of meshed sections of trunk with different resistivity.

Phase voltage of conductor, ground voltage and electrical resistivity of different sections are applied as input values to finite element analysis and the results are extracted. X component of the electric current density distribution along the cross-section of ash tree is shown in figure 10.

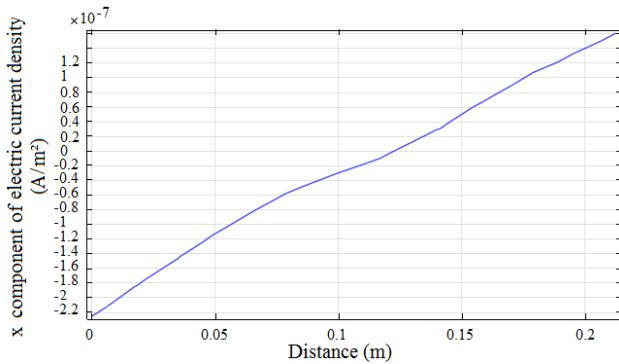


Fig. 10. Distribution of x component of the electric current density along cross-section of ash tree

Y component of the electric current density distribution along the cross-section of ash tree is presented in figure 11. As shown in figure 11, according to the variation in electrical resistivity of different sections, the current density values are not same. Figure 12 shows electric power density distribution along the cross section of ash tree at a height of 5.4 meter.

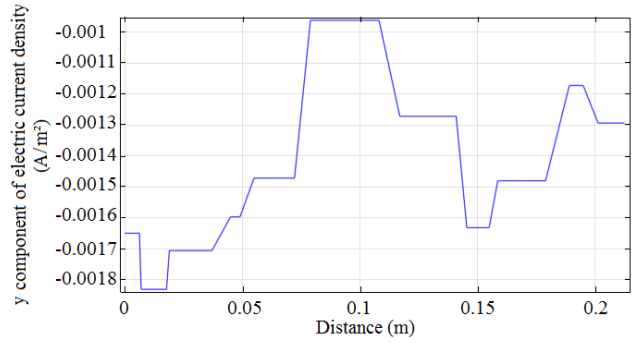


Fig. 11. y component of electric current density distribution along the cross-section of ash tree

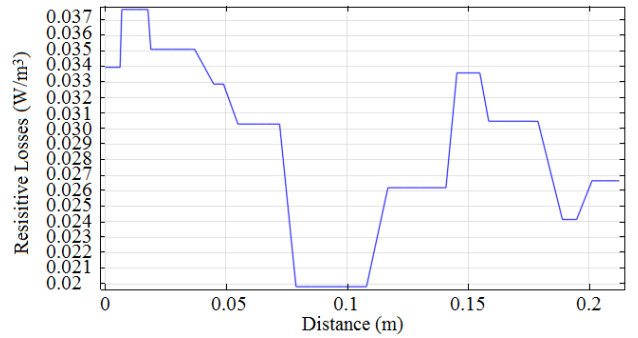


Fig. 12. Electric power density distribution along the cross section of ash tree

To verify the results obtained from two-dimensional finite element analysis with the results of the experimental tests, the values of leakage current flowing through the tree are compared with real value in two case: 1-By taking into account the total electric current of both heartwood and sapwood (Fig.). 2- By taking into account the only electric current of sapwood (Fig.). As seen, the value obtained in the second case is closer to the real value. The electrolyte content of vascular structure in tree could justify this result. It means that, passing the electric current is taken place only through the brine solution in vascular elements which plays the role of a conductor connected to the ground.

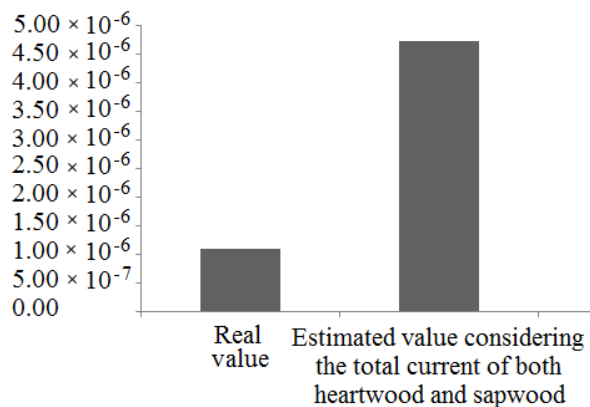


Fig. 13. Leakage current passing through trunk (A)
(Tests conducted in the spring, temperature 23 degrees, humidity 26%)

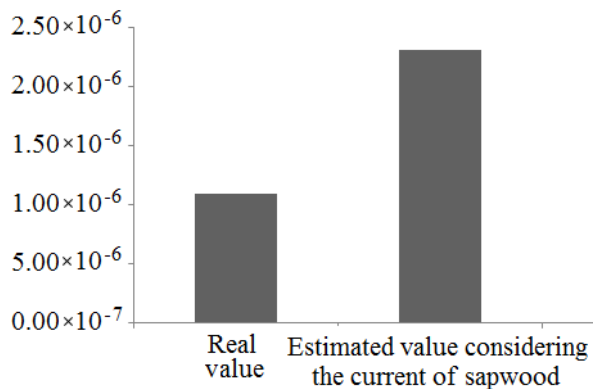


Fig. 14. Leakage current passing through trunk (A)
(Tests conducted in the spring, temperature 23 degrees, humidity 26%)

7. Conclusion

In this paper, considering this fact that the first need for the reduction of losses in distribution systems is an accurate evaluation of it, a detailed study was done on estimating of vegetation-related power losses which were so impressionable from numerous factors such as tree species, temperature, humidity and seasonal variations. In proposed methodology, using two-dimensional finite element method, the distribution of electric current and consequently the distribution of power loss along cross-section of tree trunk which was in the direct contact with LV power line was calculated. The results obtained from the proposed technique were so close to those obtained from experiments. This method also needed low computational time.

Acknowledgement

The author wishes to thank Electricity Distribution Company of Hamedan for their participation in data collection.

References

- [1] W.C. Santos, F.V. Lopes, N.S.D. Brito, B.De Souza, "High Impedance Fault Identification on Distribution Networks," *IEEE Trans. Power Deliv.* PP (99), 1–1, 2016.
- [2] A. Ghaderi, H.A. Mohammadpour, H. Ginn, Y. Shin, "High impedance fault detection in distribution network using time-frequency based algorithm," *IEEE Trans. Power Deliv.*, 30, 2014, 1260-1268..
- [3] M. Ghazizadeh-Ahsaei, "Accurate NHIF Locator Utilizing Two-End Unsynchronized Measurements," *IEEE Trans. Power Deliv.*, vol. 28, pp. 419-426, 2013.
- [4] N.I. Elkalashy, M. Lehtonen, H.A. Darwish, A.-M.I. Taalab, M.A. Izzularab, "DWT-Based Detection and Transient Power Direction-Based Location of High-Impedance Faults Due to Leaning Trees in Unearthed MV Networks," *IEEE Trans. on Power Delivery*, vol. 23, no. 1, pp. 94-101, Jan 2008.
- [5] P. Pakonen "Characteristics of partial discharges caused by trees in contact with covered conductor lines," *IEEE Trans. Dielectr. Electr. Insul.*, Vol. 15, No. 6, pp. 1626-1633, Dec. 2008.
- [6] N.I. Elkalashy, M. Lehtonen, H.A. Darwish, M.A. Izzularab, A.M.I. Taalab, "Modeling and experimental verification of high impedance arcing fault in medium voltage networks" *IEEE Trans. Dielectr. Electr. Insul.*, Vol. 14, No.2, pp. 375-383, 2007.
- [7] X. Reng, W. Ding, W. Zhou, C. Fan, and et al, "The Moisture in SF Insulated CTs Considering Current and Change of Ambient Temperature," *IEEE Trans. Power Delivery*, vol. 29, no. 3, pp. 1184 – 1191, June 2014.
- [8] F. Namdari, N. Bahador, "Modeling trees internal tissue for estimating electrical leakage current," *IEEE Trans. Dielectr. Electr. Insul.*, Vol. 23, Issue 3, pp. 1663-1674, June 2016.
- [9] A.J. Hailwood, S. Horrobin, "Absorption of water by polymers: analysis in terms of a simple model," *Trans. Faraday Soc.* Vol. 42, pp. 84–102, 1946.
- [10] H. Forsén, V. Tarvainen, "accuracy and functionality of handheld wood moisture content

mers," VTT Research Center, Espoo, Finland, 2000.

- [11] J. Fernandez-Golfin and et al, "Curves for the estimation of the moisture content of ten hardwoods by means of electrical resistance measurements" *Forest Systems*, Vol. 21, no. 1, pp. 121-127, 2012.
- [12] R. Bargallo, *Finite Elements for Electrical Engineering*, EUETIB-UPC, 2006.
- [13] S. Vázquez, E. Barocio, R. Jiménez Betancourt, "A Crank–Nicolson Galerkin approach to the analysis of electromechanical oscillations in stressed power systems," *Electric Power Systems Research*, Volume 86, May 2012, Pages 158-169.
- [14] L. Sambuelli, L.V. Socco, A. Godio, "Ultrasonic, electric and radar measurements for living trees assessment" *Bollettino di Geofisica Teorica ed Applicata*, Vol. 44, no. 3, pp. 253-279, 2003.